Cañamero, L., Oudeyer, P.-Y., and Balkenius, C. (Eds) Proceedings of the Ninth International Conference on Epigenetic Robotics: Modeling Cognitive Development in Robotic Systems. Lund University Cognitive Studies, 146.

Can imprecise internal motor models explain the ataxic hand trajectories during reaching in young infants?

Francesco Nori francesco.nori@iit.it[†]
Giulio Sandini giulio.sandini@iit.it[†]
Jürgen Konczak jkonczak@umn.edu [‡]

[†] Dep. of Robotics, Brain and Cognitive Sciences,
Italian Institute of Technology
Via Morego 30, Genova

[‡] Human Sensorimotor Control Lab.
University of Minnesota, U.S.A.
Minnesota, U.S.A.

Abstract

The first reaching movements of human infants lack limb coordination leading to ataxic-like hand trajectories. Kinematically, these early trajectories are characterized by multiple peaks in the hand velocity profile which gradually decrease in frequency during development. In this paper we explore the hypothesis that the jerky hand trajectories seen in early infancy can be the result of imprecise internal motor models. Results from our simulation suggest that imprecise estimations of multi-joint inter-segmental torques (e.g., Coriolis forces) by the controller may induce multi-peak hand velocity profiles. When the system was allowed to use delayed peripheral feedback (300 ms after reaching onset), the resulting kinematics began to resemble those seen in early infancy. This suggests that the output of an imprecise internal model of limb dynamics coupled with delayed feedback may be sufficient to explain early human hand trajectories. Our data provide an alternative to previous hypotheses theorising jerky trajectories as the result of concatenated mini ballistic movements.

1. Introduction

The first goal-directed movements of young infants at the age of 4-5 months lack coordination which gives them an ataxic appearance. The lack of proximal joint coordination leads to multiple movement units of the hand during early attempts to reach for objects (von Hofsten, 1979, Konczak et al., 1995, Berthier, 1999). That is, the hand is not moved in a smooth, stereotypical fashion, but its trajectory is jerky showing numerous changes in direction. Previous research on motor control in early infancy tried to explain this phenomenon on the basis of a faulty planning mechanism or as a compensatory motor strategy trying to overcome the lack of control (von Hofsten, 1992, Berthier, 1999). In this view, the observed segmented trajectories are a series of concatenated mini ballistic trajectories. At the end of each movement segment, the control system uses either afferent information to update the initial plan and to correct the chosen joint paths (on-line feedback control) or based on the experience from previous failures it tries not to perform a single large-amplitude reach, but executes a series of planned sub-movements. Each sub-movement is viewed as a perfect trajectory following the minimum-jerk principle (Berthier, 1999).

While such view could explain the appearance of multiple hand velocity profiles seen in infant reaching, it relies on a set of assumptions. First, the infant's motor system is seen as not being ready to deal with the peripheral bio-mechanics, but it is capable of using peripheral feedback very fast and effectively. Second, it assumes that higher cognitive structures "know" about this control predicament and induce the motor system to adapt a compensatory strategy by which a sequence of small amplitude movements are performed in order to approach a desired objects.

We here present an alternative view that may explain the phenomenon of dyscoordination in early infancy without recurrence to a cognitive mechanism. First, the assumption is made voluntary sensorimotor control is based on movement planning. Second, limb mechanics are controlled by the central nervous system. We make no specific assumption about

the exact neuroanatomical location of these control structures, although it is known that in humans they involve the motor cortices, the cerebellum, basal ganglia and the spinal cord. One way to control limb mechanics is that the neural controller has acquired an internal model of the peripheral mechanics which implies that it operates like an inverse model of the body. There is increasing empirical evidence that is consistent with the view that human motor systems uses inverse models for the multi-joint limb control (Gandolfo et al., 1996, Wolpert et al., 1998) and that these models become more precise during development (Jansen-Osmann et al., 1997). The question arises of how the infant's brain acquires an inverse model? In theory, it could be genetically determined and be operational at birth. This is unlikely knowing that early reaches show clear signs of dyscoordination, which implies that infant internal motor models at best contain imprecise estimations of the real limb parameters at birth or that the associated planning agencies are not fully functional in early infancy or both. An alternative view is that internal models are not pre-wired in the brain but are acquired through a process of parallel exploration and calibration (Metta et al., 1999). Assuming that the infant brain has acquired some form of an inverse motor model before the onset of goal-directed behaviour (e.g. through "motor babbling"), the question arises whether motor performance is susceptible to imprecise estimations of specific limb mechanical parameters. For example, given the rapid growth during the first postnatal months, could it be that an over- or underestimation of inertia or mass impacts on hand trajectory formation? The purpose of this paper is to investigate the hypothesis that early human reaching trajectories are the result of imprecise estimations of limb dynamics. We compared the simulated reaching kinematics generated by an artificial neural controller consisting of an incorrect inverse model of the human limb dynamics to the kinematics of human infants observed at the onset of goal-directed reaching (Konczak et al., 1995, Konczak and Dichgans, 1997). An incorrect controller implies that only imprecise estimations of limb mechanical parameters are available to the control system. To test the effects of an incorrect inverse model on trajectory formation, we developed a 4 degrees of freedom arm simulation that received adult-like kinematics as movement plan. Assuming a controller with a correct internal model of the arm dynamics, we show that the generated movement trajectories are identical to the planned ones. We then manipulated limb parameters such as inertia, interaction torques or gravity and compared the resulting kinematics with the planned trajectories.

Though the scope of our considerations within the current paper is limited to infant motion planning, it will be evident that the overall framework have important implications in the field of robotics, with specific concern to developmental approaches. As a matter of fact, in a wide sense, our research considers the relative role of feedback and feedforward motor control with specific attention to various stages of development.

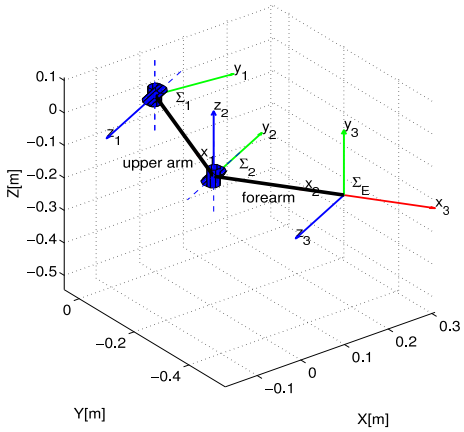

Figure 1: Three dimensional representation (using a MATLAB ® toolbox (Corke, 1996)) of the arm model kinematics in the configuration $q = [-\frac{\pi}{3}, -\frac{\pi}{3}, \frac{\pi}{3}, 0]^\top$. The shoulder and the elbow are represented by two universal joints (two degrees of freedom each). The picture shows also the link reference frames (Σ_1, Σ_2) and the end effector reference frame (Σ_E). The root reference frame Σ_o corresponds to the plot axes.

2. Method

This section describes the basic setup of the simulation. The arm model is composed of two segments, nominally the upper arm and the forearm. Each segment has two joints (two at the shoulder and two at the elbow), so that the overall structure has four degrees of freedom (see figure 1 for a sketch of the kinematic structure). The angular position of the i-th degree of freedom will be denoted q_i and the overall arm configuration $q = [q_1, q_2, q_3, q_4]^\top \in \mathbb{R}^4$. According to the Denavit-Hartenberg convention, we define an inertial reference frame Σ_o and associate two reference frames (Σ_1, Σ_2) to each of the segments (see figure 1). The rigid roto-transaltion from Σ_i to Σ_o will be denoted ${}^oT_i$ and computed as follows:

$$
\begin{aligned}
{}^oT_1 &= T_1(q_1)T_2(q_2); \\
{}^oT_2 &= T_1(q_1)T_2(q_2)T_3(q_3)T_4(q_4);
\end{aligned}
$$

i	α_i	a_i	d_i
1	0	0	0
2	$\frac{\pi}{2}$	0	0
3	0	l_1	0
4	-$\frac{\pi}{2}$	0	0

Table 1: Kinematic parameters that describes the arm forward kinematics as a function of simple anthropometric measurement, i.e. the upper arm length l_1.

with $T_i(q_i)$ represented by:

$$T_i = \begin{bmatrix} \cos_{q_i} & -\sin_{q_i} & 0 & a_i \\ \cos_{\alpha_i} \sin_{q_i} & \cos_{\alpha_i} \cos_{q_i} & -\sin_{\alpha_i} & -\sin_{\alpha_i} d_i \\ \sin_{\alpha_i} \sin_{q_i} & \sin_{\alpha_i} \cos_{q_i} & \cos_{\alpha_i} & \cos_{\alpha_i} d_i \\ 0 & 0 & 0 & 1 \end{bmatrix}, \quad (1)$$

with parameters α_i, a_i and d_i given in table 1 and computed from simple anthropometric measurement.

The differential equation used to describe the arm dynamics is the following (Murray et al., 1994):

$$M(q)\ddot{q} + C(q,\dot{q})\dot{q} + G(q) = \tau, \quad (2)$$

where $q \in \mathbb{R}^4$ is the vector of generalised coordinates (i.e. angular displacements) describing the arm posture, $\tau \in \mathbb{R}^4$ is the associated vector of generalised forces (i.e. joint torques) describing the muscle activation and M, C and G are the inertia, Coriolis and gravitational component of the dynamical forces acting on the arm. The analytical expressions for all these components have been constructed as proposed in (Yoshikawa, 1990) page 94. Their numerical values have been computed from simple anthropometric measurements following the approach proposed by (Schneider and Zernicke, 1992). The interested reader can find the complete analytical derivation in Appendix A.

2.1 Control strategy

Given the applied control strategy $\tau(t,q,\dot{q})$, $t \in [0,T]$ and the system initial condition $[q(0),\dot{q}(0)] = [q_0,\dot{q}_0]$ (typically $\dot{q}_0 = 0$), the resulting reaching movements have been simulated by integrating (2) with MATLAB SIMULINK®. Within the current framework, given a desired movement to be performed $q_d(t)$, $t \in [0,T]$ the applied control strategy is composed of a feedforward component τ_{ff} (relying on an approximation $\hat{M}$, $\hat{C}$, $\hat{G}$ of the system dynamics) and a feedback component[1] τ_{fb}:

$$\tau(t,q,\dot{q}) = \tau_{ff}(t) + \tau_{fb}(t,q,\dot{q}) \quad (3)$$

[1]In order to simplify the analysis we will not consider generic feedback gain matrices $K_p \in \mathbb{R}^{4\times4}$ and $K_v \in \mathbb{R}^{4\times4}$. We will define instead $K_p = k_p I$ and $K_v = k_v I$ where I is the 4×4 identity matrix. The effects of feedback have been evaluated by varying the scalar gains k_p and k_v in the intervals $k_p \in [0,1000]$ and $k_v \in [0,100]$.

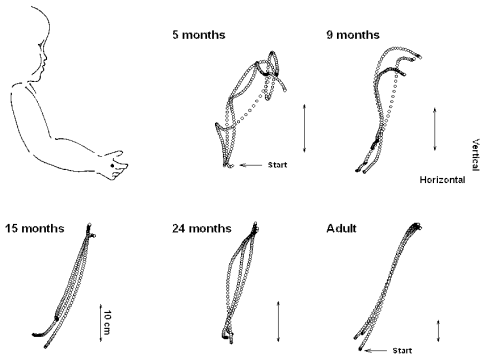

Figure 3: Exemplar hand reaching trajectories at different stages of development (Konczak and Dichgans, 1997). Remarkably, the non smooth profiles displayed by early infants are gradually replaced by straight trajectories characterized by roughly constant curvature.

where:

$$\tau_{ff}(t) = \hat{M}(q_d)\ddot{q}_d + \hat{C}(q_d,\dot{q}_d)\dot{q}_d + \hat{G}(q_d), \quad (4)$$

$$\tau_{fb}(q,\dot{q},t) = K_p(q - q_d) + K_v(\dot{q} - \dot{q}_d). \quad (5)$$

The desired trajectory $q_d(t)$, $t \in [0,T]$ (i.e., the movement plan) was extracted from a single adult goal-directed reaching movement captured at 100 Hz and interpolated with splines[2]. The use of an adult reaching profile as input for the simulation was based on the notion that it best reflected a biologically plausible movement plan.

3. Results

We systematically evaluated the effect of an imprecise controller for a wide range of incorrect dynamical parameters to obtain a sense of how sensitive the system was to imprecise estimations of inertial, gravitational and inter-segmental torques). The resulting artificial trajectories were then compared with the reaching trajectories of one human infants at different developmental stages (see Figure 2).

At first we verified that if the approximated dynamics ($\hat{M}$, $\hat{C}$, $\hat{G}$) perfectly match the system dynamics (M, C, G) then the system follows the planned trajectory, i.e. $q \equiv q_d$ (see Figure 4).

As a second step, we manipulated the feedforward component of the controller in order to visualize the effect of a mismatch between approximated and real dynamics. As shown in Figure 1 the development of reaching in humans is associated with a decrease in a

[2]The use of spline interpolation allows to obtain a continuous time function with sufficient smoothness properties for performing the double derivative operation in order to get $\dot{q}_d(\cdot)$ and $\ddot{q}_d(\cdot)$ from $q_d(\cdot)$.

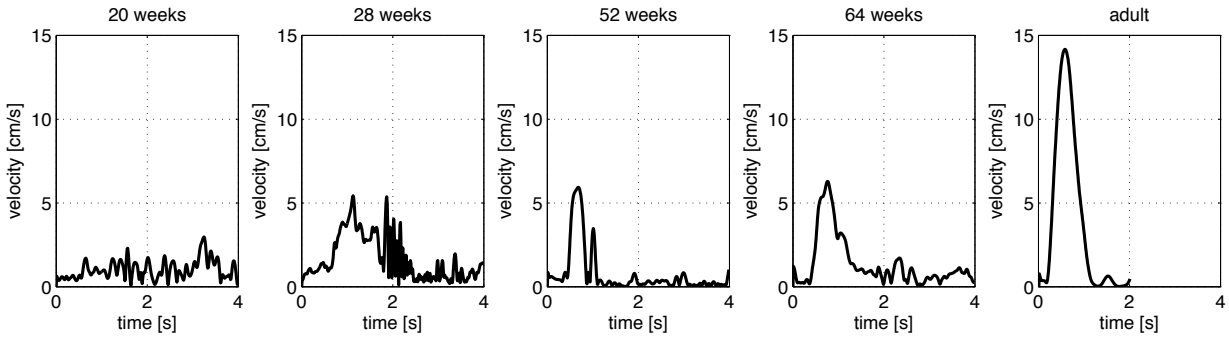

Figure 2: Exemplar 3D resultant hand velocity profiles of reaching movements at different stages of infant development (Konczak et al., 1995); the right graph shows the typical bell shaped velocity profile of an adult, which was used as movement plan.

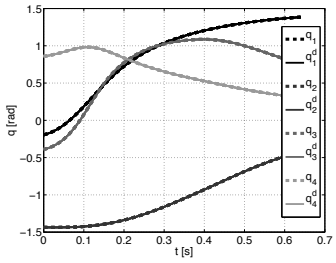

Figure 4: Joint angle trajectories corresponding to a typical reaching movement (data captured from an adult). Solid lines, q, correspond to captured data. Dashed lines, q_d, correspond to the trajectories performed when the feedforward controller perfectly inverts the dynamics of the artificial arm ($\hat{M} = M$, $\hat{C} = C$, $\hat{G} = G$). Clearly, resulting trajectories corresponded to the desired one ($q \equiv q_d$).

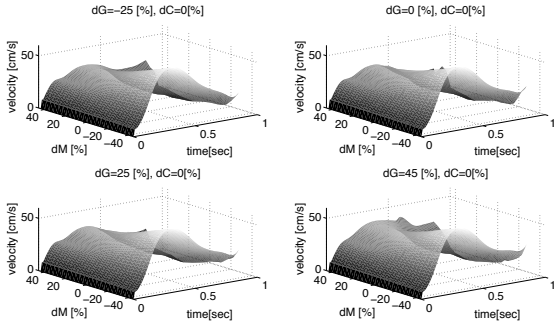

Figure 5: Effects of incorrect controllers estimates in the inertial and gravitational components ($\hat{M} \neq M$, $\hat{G} \neq G$ but $\hat{C} = C$) on the hand velocity profiles when applying a pure feedforward control ($\tau = \tau_{ff}$). Shown are four estimates of gravitational torque ($dG = -25\%$, $dG = 25\%$, $dG = 50\%$ and correct estimate $dG = 0\%$). It is evident that inaccurate gravitational and inertial component do not produce evident double peak velocity profiles.

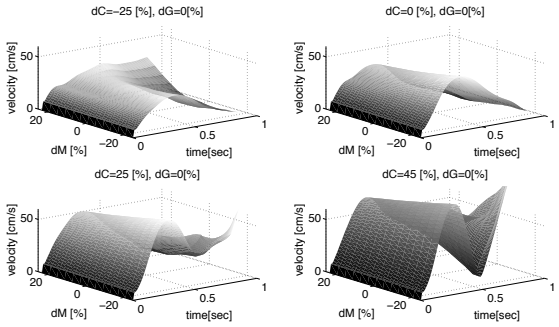

Figure 6: Four examples ($dC = -25\%$, $dC = 25\%$, $dC = 50\%$ and correct estimate $dC = 0\%$) of Coriolis forces miscalculation in a pure feedforward controller as a function of changing estimates of inertial torques. Remarkably, relevant overestimates of the Coriolis component produce double peak velocity profiles which were not present in case of inaccurate gravitational and inertial components.

the number of peaks of the hand velocity. One main result of the simulation was that similar multi-peak velocity profiles were generated when the controller values overestimated the Coriolis forces. This is evident in Figure 5 and 6 where we visualized the effects of a pure feedforward controller on the resulting hand velocity profiles. In particular, Figure 5 shows the effects of unmatched inertial and gravitational terms. The horizontal axes refer to time in seconds and percent error dM in the inertia matrix approximation:

$$\hat{M}(q) = (1 + \frac{dM}{100})M(q).$$

Vertical axis (in gray scale) represents the hand tangential velocity and the four different plots refer to different values of the percent error dG in the Coriolis component:

$$\hat{G}(q, \dot{q}) = (1 + \frac{dG}{100})G(q, \dot{q}).$$

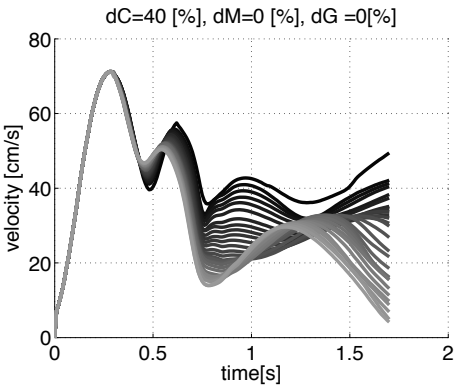

Figure 7: The effect of delayed feedback on hand trajectory formation. Shown are velocity profiles when the controller approximated dynamics did not match the Coriolis arm dynamics. ($\hat{C}$ overestimates C of a 40%). After 300 ms position feedback became available. The various profiles show the effect of different feedback gains: the darker the line the smaller the overall feedback gain $k = k_p + k_v$ is (see footnote 1 at page 3 for the definitions of k_p and k_v).

Similarly, Figure 6 shows the effects of unmatched inertial and Coriolis components with analogous definition for the percent error dC in the Coriolis component. From these pictures it is evident the hand velocity profiles remained single-peaked for incorrect estimation of the inertial and gravity components of the dynamics. In case of relevant errors in the Coriolis approximation (bottom right corner of Figure 6), multi-peak velocity profiles are generated by applying the pure feedforward component of the controller.

As a third step, we tested the effects of feedback on trajectory formation. Feedback became available after 300 ms, which approximately corresponds to delay of visual feedback in humans. It was observed that the combined effect of feedback and approximation errors in the Coriolis part of the feedback controller might result in additional velocity peaks (see Figure 7).

4. Discussion

Infants show ataxic hand trajectories with multiple movement reversals when attempting their first goal-directed reaches at around the postnatal age of 4-5 months. This observed lack of multi-joint coordination is not monocausal, but likely the result of complex interactions within the neuromuscular system. Cognitive accounts of motor development explained the lack of coordination among limb segments not primarily as a failure of a controller, but as a part of strategy of higher motor centers to overcome the deficiencies in low-level control (Berthier 1996). The results our study indicate that a neural controller with imprecise estimations of the true limb dynamics may generate ataxic endpoint trajectories that are comparable to those observed in human infants around the onset of goal-directed reaching. Especially controller overestimation of the actual Coriolis forces will induce multiple velocity profiles. The use of peripheral feedback will ensure that the hand eventually reaches the target, when the feedback gain is relatively high. It needs to be clear that these results were based on the providing a "perfect" plan to the controller. Thus, one can criticize that the results of the current simulation are limited, because this assumes that movement planning agencies in infants develop earlier than the the controller. There is no firm evidence in place to fully support this assumption. However, we here wanted to make the point that an imprecise controller alone can result in ataxic hand trajectories. Thus, the coordination deficit seen in early hand trajectory formation can be viewed as a the result of an imprecise controller with no need to assume the involvement of higher cognitive functions. The kinematic effects of an incorrect or noisy plan in conjunction with an incorrect inverse model of the plant likely enhances dyscoordination. A systematic investigation of the effect of imprecise planning on hand trajectory formation will be a next step in our series of simulations.

Acknowledgements

This work was supported by European Commission projects RobotCub (IST- 004370) and ITALK (ICT-214668).

A Dynamic equation computation

In this section we describe in details how to compute the matrices M, C and the vector G. Specifically, the (i, j) component of the matrix M denoted M_{ij} has been computed as follows:

$$M_{ij}(q) = \mathrm{tr}\left(J_{1j}(q)\hat{H}_1 J_{1i}^\top(q) + J_{2j}(q)\hat{H}_2 J_{2i}^\top(q)\right); \quad (6)$$

similarly, the i component of the vector $C\dot{q}$ (denoted h_i) has been computed as:

$$h_i(q,\dot{q}) = \sum_{j,m=1}^{4} \mathrm{tr}\left(\frac{\partial J_{1j}(q)}{\partial q_m}\hat{H}_1 J_{1i}^\top(q) + \frac{\partial J_{2j}(q)}{\partial q_m}\hat{H}_2 J_{2i}^\top(q)\right); \quad (7)$$

finally, the i component of the vector G denoted G_i is:

$$G_i(q) = -m_1 \mathbf{g}^\top J_{1i}(q) s_1 - m_2 \mathbf{g}^\top J_{2i}(q) s_2, \quad (8)$$

being $\mathbf{g}$ the gravitational vector expressed in Σ_o. In the formulas above, the matrices $\hat{H}_1$ and $\hat{H}_2$ are the

pseudo inertia matrices of the upper arm and forearm respectively; matrices J_{1i} and J_{2i} are the derivative of the rigid roto-translations ${}^oT_1$ and ${}^oT_2$:

$$J_{1i} = \frac{\partial {}^oT_1}{\partial q_i} \qquad J_{2i} = \frac{\partial {}^oT_2}{\partial q_i} \qquad i = 1, \ldots 4,$$

being q_i the i-th component of the vector q. The value of $\hat{H}_1$ and $\hat{H}_2$ depends only on s_1, s_2 (centers of mass position), m_1, m_2 (segment masses) and $\hat{I}_1$, $\hat{I}_2$ (inertia tensor of the segments with respect to the segment reference frame) according to ($k = 1, 2$):

$$\hat{H}_k = \begin{bmatrix} \frac{-\hat{I}_k^x + \hat{I}_k^y + \hat{I}_k^z}{2} & \hat{H}_k^{xy} & \hat{H}_k^{xz} & m_k s_k^x \\ \hat{H}_k^{xy} & \frac{\hat{I}_k^x - \hat{I}_k^y + \hat{I}_k^z}{2} & \hat{H}_k^{yz} & m_k s_k^y \\ \hat{H}_k^{xz} & \hat{H}_k^{yz} & \frac{\hat{I}_k^x + \hat{I}_k^y - \hat{I}_k^z}{2} & m_k s_k^z \\ m_k s_k^x & m_k s_k^y & m_k s_k^z & m_k \end{bmatrix} \quad (9)$$

The numerical values of all these quantities have been obtained from simple anthropometric measurements following the approach proposed in (Schneider and Zernicke, 1992). Specifically table 2 reports all the equations that can be used in (9) to compute $\hat{H}_1$ and $\hat{H}_2$ starting from the segments lengths (l_1, l_2), body mass (b) and segments circumference (c_1, c_2). Finally, the value of J_{ij} has been computed as:

$$\begin{aligned} J_{11} &= T_1 \Delta T_2; & J_{12} &= T_1 T_2 \Delta; \\ J_{13} &= 0; & J_{14} &= 0; \\ J_{21} &= T_1 \Delta T_2 T_3 T_4; & J_{22} &= T_1 T_2 \Delta T_3 T_4; \\ J_{23} &= T_1 T_2 T_3 \Delta T_4; & J_{24} &= T_1 T_2 T_3 T_4 \Delta; \end{aligned}$$

with T_i given as in (1) and:

$$\Delta = \begin{bmatrix} 0 & -1 & 0 & 0 \\ -1 & 0 & 0 & 0 \\ 0 & 0 & 0 & 0 \\ 0 & 0 & 0 & 0 \end{bmatrix}.$$

Similarly:

$$\begin{aligned} \frac{\partial J_{11}}{\partial q_1} &= T_1 \Delta^2 T_2; & \frac{\partial J_{11}}{\partial q_2} &= T_1 \Delta T_2 \Delta; \\ \frac{\partial J_{11}}{\partial q_3} &= 0; & \frac{\partial J_{11}}{\partial q_4} &= 0; \\ \frac{\partial J_{12}}{\partial q_1} &= T_1 \Delta T_2 \Delta; & \frac{\partial J_{12}}{\partial q_2} &= T_1 T_2 \Delta^2; \\ \frac{\partial J_{12}}{\partial q_3} &= 0; & \frac{\partial J_{12}}{\partial q_4} &= 0; \end{aligned}$$

and:

$$\begin{aligned} \frac{\partial J_{21}}{\partial q_1} &= T_1 \Delta^2 T_2 T_3 T_4; & \frac{\partial J_{21}}{\partial q_2} &= T_1 \Delta T_2 \Delta T_3 T_4; \\ \frac{\partial J_{21}}{\partial q_3} &= T_1 \Delta T_2 T_3 \Delta T_4; & \frac{\partial J_{21}}{\partial q_4} &= T_1 \Delta T_2 T_3 T_4 \Delta; \\ \frac{\partial J_{22}}{\partial q_1} &= \frac{\partial J_{21}}{\partial q_2}; & \frac{\partial J_{22}}{\partial q_2} &= T_1 T_2 \Delta^2 T_3 T_4; \\ \frac{\partial J_{22}}{\partial q_3} &= T_1 T_2 \Delta T_3 \Delta T_4; & \frac{\partial J_{22}}{\partial q_4} &= T_1 T_2 \Delta T_3 T_4 \Delta; \\ \frac{\partial J_{23}}{\partial q_1} &= \frac{\partial J_{21}}{\partial q_3}; & \frac{\partial J_{23}}{\partial q_2} &= \frac{\partial J_{22}}{\partial q_3}; \\ \frac{\partial J_{23}}{\partial q_3} &= T_1 T_2 T_3 \Delta^2 T_4; & \frac{\partial J_{23}}{\partial q_4} &= T_1 T_2 T_3 \Delta T_4 \Delta; \\ \frac{\partial J_{24}}{\partial q_1} &= \frac{\partial J_{21}}{\partial q_4}; & \frac{\partial J_{24}}{\partial q_2} &= \frac{\partial J_{22}}{\partial q_4}; \\ \frac{\partial J_{24}}{\partial q_3} &= \frac{\partial J_{23}}{\partial q_4}; & \frac{\partial J_{24}}{\partial q_4} &= T_1 T_2 T_3 T_4 \Delta^2. \end{aligned}$$

References

Berthier, N. E. (1999). Learning to reach: A mathematical model. *Developmental Psychology*, 32:811–823.

Corke, P. (1996). A robotics toolbox for MATLAB. *IEEE Robotics and Automation Magazine*, 3(1):24–32.

Gandolfo, F., Mussa-Ivaldi, F. A., and Bizzi, E. (1996). Motor learning by the field approximation. In *Proceedings of the National Academy of Science*, volume 93, pages 3843–3846.

Jansen-Osmann, P., Richter, S., Konczak, J., and Kalveram, K. (1997). Force adaptation transfers to untrained workspace regions in children: Evidence for developing inverse dynamic models. *Experimental Brain Research*, 143:212–220.

Konczak, J., Borutta, M., Topka, H., and Dichgans, J. (1995). Development of goal-directed reaching in infants: Hand trajectory formation and joint force control. *Experimental Brain Research*, 106:156–168.

Konczak, J. and Dichgans, J. (1997). Goal-directed reaching: development toward stereotypic arm kinematics in the first three years of life. *Experimental Brain Research*, 117:346–354.

Metta, G., Sandini, G., and Konczak, J. (1999). A developmental approach to visually-guided reaching in artificial systems. *Neural Networks*, 12:1413–1427.

Upper	m_1	$=$	$1.2249 \times 10^{-2} b + 1.3067 \times 10^{0} l_1 + 9.8645 \times 10^{-1} c_1 - 1.9376 \times 10^{-1}$
	I_1	$=$	$\begin{bmatrix} 0 & 0 & 0 \\ 0 & \frac{m_1 l_1^2}{3} & 0 \\ 0 & 0 & \frac{m_1 l_1^2}{3} \end{bmatrix}$
	$\hat{I}_1$	$=$	$\begin{bmatrix} \hat{I}_2^x & -\hat{H}_2^{xy} & -\hat{H}_2^{xz} \\ -\hat{H}_2^{xy} & \hat{I}_2^y & -\hat{H}_2^{yz} \\ -\hat{H}_2^{xz} & -\hat{H}_2^{yz} & \hat{I}_2^z \end{bmatrix}$
		$=$	$I_1 + m_1 \begin{bmatrix} 0 & -s_k^z & s_k^y \\ s_k^z & 0 & -s_k^x \\ -s_k^y & s_k^x & 0 \end{bmatrix}$
	s_1	$=$	$\begin{bmatrix} s_1^x \\ s_1^y \\ s_1^z \end{bmatrix} = \begin{bmatrix} 0.4428 \times l_1 \\ 0 \\ 0 \end{bmatrix}$
Fore	m_2	$=$	$5.2671 \times 10^{-3} b + 9.7584 \times 10^{-1} l_2 + 1.1492 \times 10^{0} c_2 - 1.6886 \times 10^{-1}$
	I_2	$=$	$\begin{bmatrix} 0 & 0 & 0 \\ 0 & \frac{m_2 l_2^2}{3} & 0 \\ 0 & 0 & \frac{m_2 l_2^2}{3} \end{bmatrix}$
	$\hat{I}_2$	$=$	$\begin{bmatrix} \hat{I}_2^x & -\hat{H}_2^{xy} & -\hat{H}_2^{xz} \\ -\hat{H}_2^{xy} & \hat{I}_2^y & -\hat{H}_2^{yz} \\ -\hat{H}_2^{xz} & -\hat{H}_2^{yz} & \hat{I}_2^z \end{bmatrix}$
		$=$	$I_2 + m_2 \begin{bmatrix} 0 & -s_2^z & s_2^y \\ s_2^z & 0 & -s_2^x \\ -s_2^y & s_2^x & 0 \end{bmatrix}$
	s_2	$=$	$\begin{bmatrix} s_2^x \\ s_2^y \\ s_2^z \end{bmatrix} = \begin{bmatrix} 0.4541 \times l_2 \\ 0 \\ 0 \end{bmatrix}$

Table 2: Dynamical parameters as a function of simple anthropometric measurements (Schneider and Zernicke, 1992): $b[kg]$ = infant body mass ; $l_k[m]$ = segment length; $c_k[m]$ = segment circumference. Values of these anthropometric measurements have been measured on subjects. Dynamical parameters have been computed accordingly: $m_k[kg]$ = segmental mass; $s_k[m]$ = center of mass position with respect to the segment reference frame; $I_k[kg \cdot m^2]$ = inertia tensor with respect to the frame with its origin at the center of mass. Note that in the calculation of the inertia tensors segments have been approximated with one dimensional rods.

Murray, R. M., Li, Z., and Sastry, S. S. (1994). *A Mathematical Introduction to Robotic Manipulation*. CRC Press.

Schneider, K. and Zernicke, R. (1992). Mass, center of mass, and moment of inertia estimates for infant limb segments. *Jouranl of Biomechanics*, 25:145–148.

von Hofsten, C. (1979). Development of visually directed reaching: the approach phase. *Journal of Human Movement Studies*, 5:160–178.

von Hofsten, C. (1992). *The gearing of early reaching to the environment.*, volume 87. Elsevier, Amsterdam.

Wolpert, D. M., Miall, R. C., and Kawato, M. (1998). Internal models in the cerebellum. *Trends in Cognitive Sciences*, 2:338–347.

Yoshikawa, T. (1990). *Foundations of Robotics: Analysis and Control*. MIT Press.